



# CHORUS

This is the accepted manuscript made available via CHORUS. The article has been published as:

## Unified Theoretical Framework for Polycrystalline Pattern Evolution

Ari Adland, Yechuan Xu, and Alain Karma

Phys. Rev. Lett. **110**, 265504 — Published 25 June 2013

DOI: [10.1103/PhysRevLett.110.265504](https://doi.org/10.1103/PhysRevLett.110.265504)

# Unified Theoretical Framework for Polycrystalline Pattern Evolution

Ari Adland,<sup>1</sup> Yechuan Xu,<sup>1</sup> and Alain Karma<sup>1</sup>

<sup>1</sup>*Physics Department and Center for Interdisciplinary Research on Complex Systems, Northeastern University, Boston, MA 02115*

(Dated: May 13, 2013)

The rate of curvature-driven grain growth in polycrystalline materials is well-known to be limited by interface dissipation. We show analytically and by simulations that, for systems forming modulated phases or non-equilibrium patterns with crystal ordering, growth is limited by bulk dissipation associated with lattice translation, which dramatically slows down grain coarsening. We also show that bulk dissipation is reduced by thermal noise and that this reduction leads to faster coarsening behavior dominated by interface dissipation for high Peierls barrier and high noise. Those results provide a unified theoretical framework for understanding and modeling polycrystalline pattern evolution in diverse systems over a broad range of length and time scales.

PACS numbers: 61.72.Mm, 05.40.Ca, 61.72.Hh, 62.20.Hg

Polycrystalline patterns are observed in very diverse systems including crystalline solids [1], colloidal systems [2, 3], various spatially modulated phases of macromolecular systems such as diblock copolymers [4, 5], and non-equilibrium (NE) dissipative structures [6]. When grain boundaries (GBs) between domains of different crystal orientation are mobile, those patterns generally coarsen in time to reduce GB length or area by elimination of smaller grains. This coarsening behavior has been extensively studied because of its practical importance for engineering polycrystalline materials [7] and its fundamental relevance for our general understanding of nonequilibrium ordering phenomena.

The two-dimensional (2D) ordering dynamics of modulated phases and NE patterns has been investigated theoretically [8–16] in the framework of model equations of the general variational form

$$p\partial_t^2\psi + \alpha\partial_t\psi = -(-\nabla^2)^n \frac{\delta\mathcal{F}}{\delta\psi} + \eta, \quad (p, n = 0 \text{ or } 1), \quad (1)$$

where  $\psi$  is an order parameter appropriate to each system that can be globally conserved ( $n = 1$ ) or non-conserved ( $n = 0$ ), and  $\eta$  is a noise uncorrelated in space and time with a variance determined by the fluctuation-dissipation relation  $\langle\eta(\vec{r}, t)\eta(\vec{r}', t')\rangle = 2\alpha T(-\nabla^2)^n\delta(\vec{r} - \vec{r}')\delta(t - t')$ . The form (1) insures that the system relaxes to a global minimum of the Lyapounov functional  $\mathcal{F}$  corresponding to the lattice ordered state. Eq. (1) has also emerged as fruitful computational framework –the phase-field-crystal (PFC) approach [17, 18]– to model polycrystalline materials on diffusive time scales with  $\psi$  interpreted as the crystal density field. While Eq. (1) has been traditionally studied for purely relaxational ( $p = 0$ ) dynamics [8–17], propagative ( $p = 1$ ) wave-like dynamics have also been introduced in the PFC context to mimic phonon-mediated relaxation of the strain field [18].

Experimental studies of modulated phases [4] and extensive computational studies of Eq. (1) have shown that the characteristic grain size of 2D hexagonal lattices

[13–16] grows  $\sim t^q$ . The exponent  $q$  is typically much smaller than the  $q = 1/2$  value expected for “normal grain growth” in polycrystalline materials [19, 20], and depends on parameters and noise strength [15, 16]. While there have been theoretical attempts to explain those exponents for roll patterns [9–12], the origin of this sluggish (low  $q$ ) coarsening kinetics is still poorly understood for two-dimensional lattices with crystal-like ordering.

In this letter, we show that the sluggish ordering dynamics of 2D crystal lattices results from the subtle effect of “bulk” dissipation. To highlight the origin of this effect, consider for simplicity the case of non-conserved dynamics (the same effect is present for conserved dynamics). For this case, Eq. (1) implies that

$$\frac{d}{dt}[\mathcal{F} + E_k] = - \int d\vec{r} \alpha(\partial_t\psi)^2, \quad (2)$$

where  $E_k \equiv p \int d\vec{r} (\partial_t\psi)^2/2$  is the kinetic energy of phonon-like modes. Since the relaxation of the elastic field is fast compared to grain coarsening, it follows that  $|dE_k/dt| \ll |d\mathcal{F}/dt|$ . Therefore the left-hand-side of Eq. (2)  $\approx d\mathcal{F}/dt$ , which is the rate of decrease of the total excess GB free-energy in the polycrystal. For solids, this excess free-energy is dissipated through GB motion during grain growth. Importantly, grain growth has also been shown to be accompanied by grain rotation [21–24]. However, for solids, this rotation does not produce any dissipation in the grain interior owing to the Galilean invariance of Newton’s second law, which governs the motion of real atoms in a crystal. In contrast, for continuous lattice patterns, “pseudo atoms” correspond to peaks of the  $\psi$  field, whose evolution is governed by Eq. (1) that is not Galilean invariant. Hence grain rotation induces a local lattice translation that makes  $\partial_t\psi$  non-vanishing in the grain interior, thereby contributing to the dissipation of the GB free-energy through the right-hand-side (r.h.s) of Eq. (2). This “bulk” dissipation can influence the rate of grain growth in addition to interface dissipation associated with the  $\psi$ -dynamics in GB regions. Our main

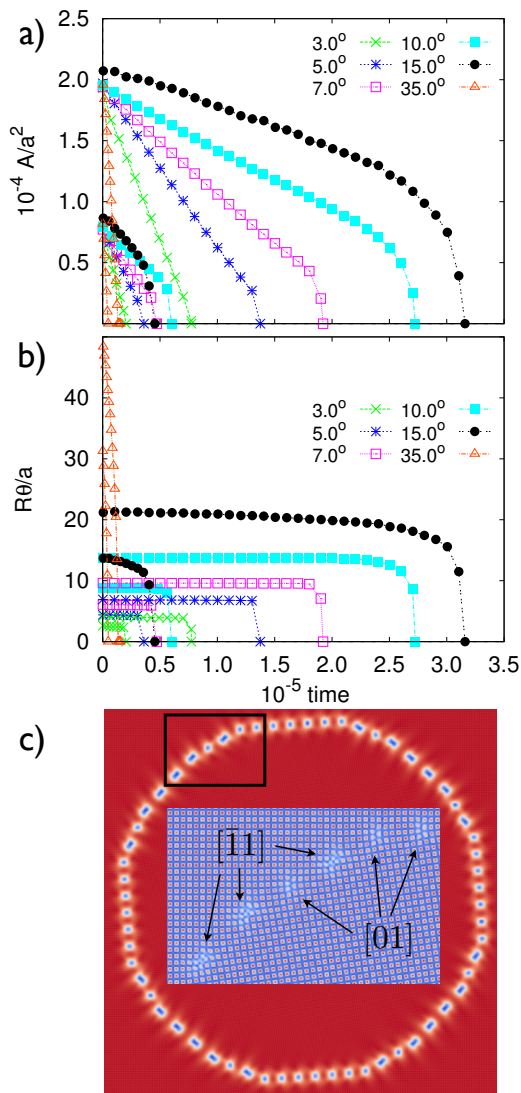


Figure 1: Results of embedded grain simulations for  $\epsilon = 0.12$  and  $T = 0$  showing normalized grain area (a) and  $R\theta/a$  (b) versus time for two different initial grain areas and six different initial misorientations. Grain rotation is present (absent) for misorientation less (larger) than  $\sim 15^\circ$ . (c) order parameter  $\phi$  defined by Eq. (7) for the largest area  $7^\circ$  simulation showing the GB structure, with  $\langle 11 \rangle$  ( $\langle 10 \rangle$ ) dislocation cores appearing as elongated (circular) blue patches, and the corresponding  $\psi$  field inside the square region (inset).

finding is that bulk rather than interface dissipation can dictate the rate of grain growth for lattice patterns governed by Eq. (1) in the limit of small Peierls-Nabarro (PN) barrier to dislocation motion and small noise. We also demonstrate the existence of a non-trivial cross-over from bulk- to interface-dominated dissipation with increasing PN barrier and noise strength.

To show this, we first solve analytically the problem of the shrinkage of an embedded circular grain in a single crystal matrix for  $n = 0$ . In this analysis, we keep  $p$  ar-

bitrary to show explicitly that phonon-like modes have a negligible contribution, so that the  $p = 0$  and  $p = 1$  dynamics exhibit similar behaviors. We then validate this solution and explore the coarsening behavior of multi-grain structures. We simulate both Eq. (1) and a modified version of Eq. (1) with minimized bulk dissipation (MBD). The latter is shown to yield a different coarsening behavior dominated by interface dissipation representative of crystalline solids. Furthermore, for concreteness, we carry out our simulations for  $p = 1$  and  $n = 0$  and use a PFC form of  $\mathcal{F} = \int d\vec{r} \omega$ , which favors a square-lattice in 2D with the choice [27, 28]

$$\omega = \psi [-\epsilon + (\nabla^2 + 1)^2 (\nabla^2 + 2)^2] \psi / 2 + \psi^4 / 4 - \mu \psi. \quad (3)$$

This model was recently shown to produce GBs with a similar dislocation content as  $[001]$  tilt GBs in molecular dynamics (MD) simulations of face-centered-cubic bi-crystals [29]. In the analogy with a crystal-liquid system,  $\mathcal{F}$  is the grand potential that is equal in the crystal and liquid ( $\psi = 0$ ) phases for an equilibrium value of the chemical potential  $\mu = \mu_E$  [28], which depends generally on both  $\epsilon$  and noise strength  $T$ . We note that  $T$  represents physically an effective temperature in the PFC model since short-wavelength fluctuations on the lattice scale are already partly accounted for in the bare form of  $\mathcal{F}$ . Here we choose the values  $\mu = -0.90$  for  $\epsilon = 0.12$  and  $\mu = -1.69$  for  $\epsilon = 0.5$ . This choice insures that the system remains inside the stable solid region for both zero and finite noise values studied here [31]. Since the height of the PN barrier scales  $\sim \exp(-c/\epsilon^{1/2})$  where  $c$  is some constant (see, e.g. [12]), the height decreases rapidly with decreasing  $\epsilon$ . For  $\epsilon = 0.12$ , this height is very small so that curvature-driven grain growth occurs at  $T = 0$ , while for  $\epsilon = 0.5$  the barrier is large enough to pin GBs that only become mobile for finite  $T$ .

*Embedded grain theory.* Consider a circular grain of radius  $R(t)$  and misorientation  $\theta(t)$  with respect to its surrounding single crystal matrix. For small initial misorientation  $\theta(0)$ , grain rotation is geometrically necessary under the assumption that the number of dislocations along the GB is conserved, as highlighted by Cahn and Taylor in the context of solids [22]. Since there are  $n_d = 2\pi R\theta/b$  dislocations of Burgers vector magnitude  $b$ , this conservation condition implies that

$$R(t)\theta(t) = R(0)\theta(0), \quad (4)$$

and hence that the embedded circular grain rotates towards larger misorientation as it shrinks. This rotation can also be interpreted as a consequence of the geometrical coupling between GB motion and a shear stress [22, 25, 26]. In addition to Eq. (4), we need a dynamical equation to prescribe the dynamics of both  $R(t)$  and  $\theta(t)$ . This equation can be obtained readily by evaluating each term in the relaxation equation (2) for a circular grain. The time rate of change of total GB en-

ergy is  $\dot{\mathcal{F}} = d[2\pi R(t)\gamma(\theta(t))]/dt$  where  $\gamma(\theta)$  is the energy per unit length of GB and dot denotes derivative with respect to time. To evaluate separately the contributions of interface and bulk dissipation, we write the integral on the r.h.s. of Eq. (2) as the sum  $\int = \int_I + \int_B$ , where the interface contribution  $\int_I$  is evaluated over a thin annulus comprising the GB (of thickness proportional to the dislocation core radius) and the bulk contribution  $\int_B$  is evaluated over the entire embedded grain area. Dislocations move radially inward by pure glide at a velocity  $\dot{R}$ , and hence  $|\partial_t \psi| \sim a^{-1} \dot{R}$  over an area  $a^2$  around each dislocation, where  $a$  is the lattice spacing. Therefore, the total interface dissipation  $\int_I d\vec{r} \alpha (\partial_t \psi)^2 = n_d a^2 \alpha (a^{-1} \dot{R})^2 / m = \alpha 2\pi R \dot{R}^2 \theta / (mb)$ , where  $m$  is an  $O(1)$  dimensionless prefactor. This yields the expression for the mobility  $M(\theta) = mb/(\alpha\theta)$  for  $\theta \ll 1$  in agreement with the Cahn-Taylor prediction for solids [22] recently validated by MD simulations [26].

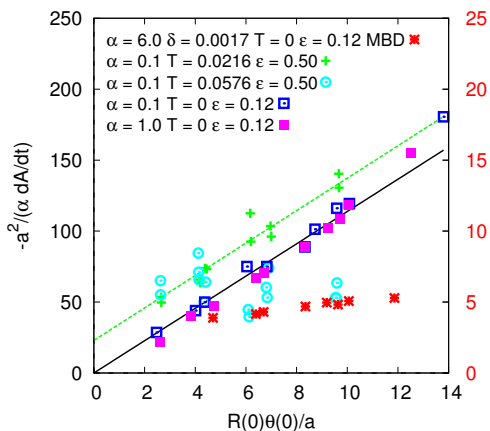


Figure 2: Comparison of theory for the octagonal grain shown as a black solid (green dashed) line for  $\epsilon = 0.12$  ( $\epsilon = 0.5$ ), and simulations of Eq. (1) (symbols); the slopes  $s_2 K a / E_0$  are predicted by Eq. 6. The fitted intercept for the green dashed line represents a finite contribution of interface dissipation for intermediate noise. Red star symbols are for the modification of Eq. (1) with minimized bulk dissipation (MBD), which causes the grain shrinkage rate to become independent of grain size and misorientation for small misorientation.

Next, to compute the bulk dissipation rate  $\int_B d\vec{r} \alpha (\partial_t \psi)^2$ , we compute the dissipation rate per unit area of a crystal field in uniform translation at velocity  $\vec{v}$  and then integrate the result over the entire grain area. In a region in uniform translation,  $\psi(\vec{r}, t) \approx \psi_0(\vec{r} - \vec{v}t)$ , where  $\psi_0(\vec{r})$  is the equilibrium  $\psi$ -field that minimizes  $\mathcal{F}$ , and hence  $\partial_t \psi = -\vec{v} \cdot \vec{\nabla} \psi_0$ . The dissipation rate per area of crystal can therefore be written in the form  $\alpha K v^2 / A_{u.c.}$  where  $K \equiv \int_{u.c.} d\vec{r} (\hat{v} \cdot \vec{\nabla} \psi_0)^2$  is computed over the area  $A_{u.c.}$  of one unit cell (u.c.). For a square lattice,  $A_{u.c.} = a^2$  and  $K$  is independent

of the direction of  $\hat{v}$  relative to the crystal axes, and reduces to  $K = \int_0^a \int_0^a dx' dy' (\partial_{x'} \psi_0)^2$  where  $x'$  and  $y'$  are the principal crystal axes. Since  $v = r\dot{\theta}$  in each small region of a large rotating grain, where  $r$  is the radial polar coordinate, the total bulk dissipation rate is obtained by integrating  $\alpha K v^2 / A_{u.c.}$  over the grain area:  $\int_0^R 2\pi r dr \alpha K (r\dot{\theta})^2 / a^2 = \alpha \pi K R^4 \dot{\theta}^2 / (2a^2) = 2\alpha E_k$ . Combining the above expressions for interface and bulk dissipation, Eq. (2) becomes

$$\dot{R}\gamma + R\gamma\dot{\theta} = -\alpha R \dot{R}^2 \theta / (mb) - \alpha K R^4 \dot{\theta}^2 / (4a^2), \quad (5)$$

where we have neglected  $\dot{E}_k$  which can be shown to give a negligible higher order contribution. Thus the  $p = 0$  and  $p = 1$  dynamics in Eq. (1) yield the same grain rotation dynamics. Finally, approximating the GB energy with a Read-Shockley (RS) law  $\gamma(\theta) = E_0 \theta (A_c - \ln \theta)$  valid for small  $\theta$ , and using the condition  $R(t)\theta(t) = R(0)\theta(0)$  that  $n_d$  is conserved, Eq. (5) yields a single dynamical equation for  $R(t)$  that can be analytically solved. Its solution predicts that the grain area ( $A = \pi R^2$ ) decreases linearly in time with a rate  $\dot{A} = dA/dt$  given by

$$-a^2 / (\alpha \dot{A}) = s_1 a^2 / (mb E_0) + s_2 K R(0) \theta(0) / E_0, \quad (6)$$

where  $s_1 = 1/(2\pi)$  and  $s_2 = 1/(8\pi)$ , and the first and second terms on the r.h.s. correspond to interface and bulk dissipation, respectively. Since  $b \sim a$  and  $m$  and  $K$  are constants of order unity, Eq. (6) predicts that the ratio of bulk to interface dissipation is  $\sim R(0)/a \gg 1$ , implying that  $\dot{A}$  is entirely dominated by bulk dissipation, which holds for any lattice structure.

*Embedded grain simulations.* To test Eq. (6), we simulated embedded grains using Eq. (1) with  $\mathcal{F}$  defined by Eq. (3). We used a pseudo-spectral method described in [30] with more details given in [31]. Fig. 1 shows plots of grain area and  $R\theta/a$  versus time together with a snapshot that highlights the structure of the GB, consisting of dislocations with Burgers vectors described by the Miller indices  $\langle 11 \rangle$  and  $\langle 10 \rangle$ . Accordingly, the grain is approximately shaped as an octagon with 4 facets made up of  $[11]$ ,  $[\bar{1}1]$ ,  $[1\bar{1}]$ , and  $[\bar{1}\bar{1}]$  dislocations, and 4 others with  $[10]$ ,  $[01]$ ,  $[\bar{1}0]$ , and  $[0\bar{1}]$  dislocations, respectively. Fig. 1a shows that  $\dot{A}$  is constant and depends on both initial grain size and misorientation, and that  $R\theta$  is constant; the number of dislocations is conserved until dislocations annihilate during the final stage of grain collapse. In Fig. 2, we compare quantitatively  $\dot{A}$  values extracted from linear fits of  $A$  vs. time plots (before grain collapse) to the predictions of Eq. (6) extended to an octagonal grain with two dislocation types:  $E_0 = (E_0^{11} + E_0^{10})/2$  and  $(mb)^{-1} = [(m_{10}b_{10})^{-1} + (m_{11}b_{11})^{-1}]/2$ , where  $s_1 = 1/(4\sqrt{2})$  and  $s_2 = 0.0368$  are related to the perimeter and area of an octagon and  $E_0^{11}$  and  $E_0^{10}$  are extracted from fits of computed GB free-energies to a RS law [31]. This comparison shows an excellent quantitative agreement

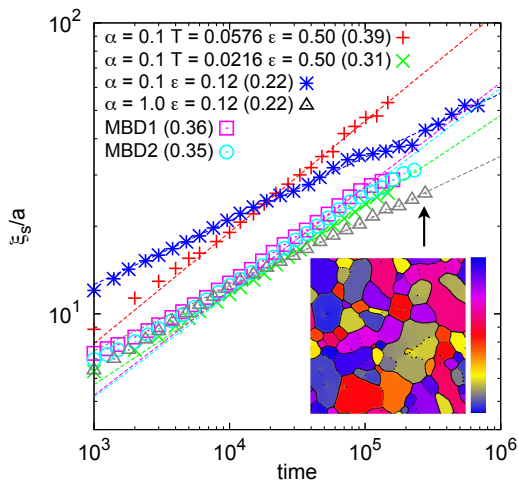


Figure 3: Plot of ordering length  $\xi_S$  ( $\sim$  mean grain size) vs. time from simulations of Eq. (1) (parameters in legends) and minimized bulk dissipation with  $\epsilon = 0.12$ ,  $\alpha = 8$ , and  $\delta = 3.1 \cdot 10^{-3}$  ( $\delta = 6.3 \cdot 10^{-3}$ ) for MBD1 (MBD2);  $T = 0$  when not given in legend. Numbers in parentheses are growth exponents from straight-line fits at large times (dashed lines). Inset: orientation field computed using a wavelet transform of  $\psi$  with a color bar ranging from  $-45^\circ$  to  $45^\circ$  [31].

for  $\epsilon = 0.12$  and  $T = 0$  for two different  $\alpha$  values, confirming that inertia ( $p = 1$ ) is unimportant. The comparison for  $\epsilon = 0.5$  with large PN barrier shows that bulk dissipation is still dominant for intermediate  $T$  ( $T = 0.0216$ ). The slope of the curve predicted by Eq. (6) fits well the simulation results, but the curve has a finite intercept at the origin corresponding to a finite contribution of interface dissipation. This contribution is negligible for  $\epsilon = 0.12$  where the intercept merges with the origin. For  $\epsilon = 0.5$  and larger  $T$  ( $T = 0.0576$ ), bulk dissipation is reduced and the simulation data is no longer fitted by the theory. Analysis of dislocation dynamics in the simulations shows that this reduction results from thermally activated dislocation reactions. Those reactions reduce the number of dislocations, thereby allowing the grain to shrink with less rotation and reducing the contribution of bulk dissipation relative to interface dissipation. Reduction of grain rotation by dislocation reaction is also observed in MD simulations of grain rotation [24].

*Grain growth simulations.* Next we simulated Eq. (1) with  $p = 1$  and  $n = 0$  in large systems of  $512 \times 512$  unit cells with periodic boundary conditions. We seeded in a liquid a large number of small randomly oriented grains, which crystallize into a very fine grain polycrystal. We then characterized the coarsening of this polycrystal by measuring the ordering scale  $\xi_S$  using the half width  $\delta k$  at half peak of the structure factor  $S(k, t) = \langle \psi(\vec{k}, t) \psi^*(\vec{k}, t) \rangle$  (fitted to a squared Lorentzian), where the angular brackets denote averages over all orientations of  $\vec{k}$  in the same simulation [10, 31]. Plots of  $\xi_S \equiv \delta k^{-1}$

vs. time in Fig. 3 for simulations of Eq. (1) with  $\epsilon = 0.12$  and  $T = 0$  yield a small coarsening exponent  $q \approx 0.22$  as in previous experimental [4] and computational [13–16] studies of 2D hexagonal lattices.

To test the hypothesis that this sluggish coarsening kinetics results from bulk dissipation, we simulated a modified MBD version of Eq. (1) where dissipation is minimized in the bulk and localized at GBs. This is achieved by the substitution  $\alpha \rightarrow \alpha h(\phi)$  in Eq. (1) where

$$\phi(\vec{r}) = C \int d\vec{r}' \exp(-|\vec{r} - \vec{r}'|^2 / 2\zeta^2) |\nabla \psi(\vec{r}')|^2 \quad (7)$$

is a spatially varying order parameter directly analogous to the conventional phase field for crystal ordering [32]. We choose  $\zeta = a/2$  and the normalization constant  $C$  such that  $\phi$  is unity in ordered regions of the lattice and decreases below unity in dislocation cores and GBs, as illustrated in Fig. 1c for the embedded grain. The function  $h(\phi)$  given in [31] has limits  $h(1) = \delta$  and  $h(\phi) \sim O(1)$  in ordered and disordered regions, respectively, thereby allowing us to minimize the ratio of bulk and interface dissipation by choosing  $\delta \ll 1$ . To test the MBD dynamics, we first repeated the single embedded grain simulations. The results in Fig. 2 (red stars) show that the grain shrinkage rate becomes independent of initial grain size and misorientation as in MD simulations [24]. This result is consistent with the theoretical prediction that, for MBD, the second term on the r.h.s. of Eq. (6) corresponding to bulk dissipation is multiplied by  $\delta$  and hence becomes negligible in the limit  $\delta \ll 1$ .

Next, we repeated the multi-grain simulations with MBD dynamics. The results in Fig. 3 show that MBD yields a larger exponent  $q \approx 0.35$  than  $q \approx 0.22$  for standard PFC dynamics (1), thereby demonstrating that bulk dissipation significantly slows down the coarsening kinetics even though grain rotation is more constrained in a complex GB network. This conclusion is further supported by the finding that grain rotation is more prevalent in MBD than standard PFC simulations and by computing the ratio of interface and total dissipation. This ratio decreases to a small value with standard PFC dynamics but remains approximately unity with MBD [31]. Finally, simulations for  $\epsilon = 0.5$  show that the growth exponent increases markedly with  $T$ , as expected from the reduction of bulk dissipation by dislocation reactions. More important here than the precise values of the exponents, which are not exactly constant in time, is the demonstration of the key role of bulk dissipation in the ordering dynamics of 2D lattice forming systems.

The present results should be testable experimentally in a wide range of systems forming modulated phases or NE patterns with crystal ordering. They also highlight the necessity of reformulating the PFC dynamics for realistically modeling polycrystalline materials.

This work was supported by US DOE grants DE-FG02-07ER46400.

- 
- [1] A. P. Sutton and R. W. Balluffi, *Interfaces in Crystalline Materials* (Clarendon Press, Oxford, 1995).
- [2] K. Yoshizawa, T. Okuzono, T. Koga, T. Taniji, and J. Yamana, *Langmuir* **27**, 13420 (2011).
- [3] S. Gokhale, K. Hima Nagamasab, V. Santhoshc, A. K. Sooda, and Rajesh Ganapathyc, *Proc. Natl. Acad. Sci.* **109**, 20314 (2012).
- [4] C. Harrison, D. E. Angelescu, M. Trawick, Z. Cheng, D. A. Huse, P. M. Chaikin, D. A. Vega, J. M. Sebastian, R. A. Register and D. H. Adamson, *Europhys. Lett.*, **67** 800 (2004).
- [5] S. Ji, C.C. Liu, W. Liao, A. L. Fenske, G. S. W. Craig, P. F. Nealey, *Macromolecules* **44** 4291 (2011).
- [6] M. C. Cross and H. Greenside, *Pattern Formation and Dynamics in Nonequilibrium Systems* (Cambridge University Press, 2009).
- [7] E. A. Holm and S. M. Foiles, *Science* **328**, 1138 (2010).
- [8] J. Swift and P. C. Hohenberg, *Phys. Rev. A* **15**, 319 (1977).
- [9] K. R. Elder, J. Vinals, and M. Grant, *Phys. Rev. Lett.* **68**, 3024 (1992).
- [10] M. C. Cross and D. I. Meiron, *Phys. Rev. Lett.* **75**, 2152 (1995).
- [11] Q. Hou, S. Sasa, and N. Goldenfeld, *Physica A* **239**, 219-226 (1997).
- [12] D. Boyer and J. Vinals, *Phys. Rev. E* **64** 050101(R) (2001).
- [13] D. Boyer and J. Vinals, *Phys. Rev. Lett.* **89**, 055501 (2002).
- [14] D. A. Vega, C. K. Harrison, D. E. Angelescu, M. L. Trawick, D. A. Huse, P. M. Chaikin, R. A. Register *Phys. Rev. E* **71**, 061803 (2005).
- [15] L. R. Gomez, E. M. Valles, and D. A. Vega, *Physica A* **386**, 648 (2007).
- [16] H. Ohnogi and Y. Shiwa, *Phys. Rev. E* **84**, 051603 (2011).
- [17] K. R. Elder, M. Katakowski, M. Haataja, and M. Grant, *Phys Rev Lett* **88**, 245701 (2002); K. R. Elder and M. Grant, *Phys Rev E* **70**, 051605 (2004); J. Berry, M. Grant and K. R. Elder, *Phys Rev E* **73**, 031609 (2006).
- [18] P. Stefanovic, M. Haataja, and N. Provatas, *Phys Rev Lett* **96**, 225504 (2006).
- [19] The ideal grain growth 1/2 exponent follows dimensionally from the proportionality relation between GB velocity and curvature and the assumption of a self-similar coarsening behavior (see, e.g. [20]).
- [20] W. W. Mullins and J. Vinals. *Acta Metall.* **37**, 991 (1989).
- [21] M. Upmanyu, D.J. Srolovitz, A.E. Lobkovsky, J.A. Warren, W.C. Carter, *Acta Mater.* **54** 1707 (2006).
- [22] J. W. Cahn and J. E. Taylor, *Acta Mater.* **52**, 4887 (2004).
- [23] K.-A. Wu, and P. W. Voorhees, *Acta Mater.* **60**, 407 (2012).
- [24] Z. T. Traut and Y. Mishin, *Acta Mater.* **60**, 2407 (2012).
- [25] J. W. Cahn, Y. Mishin, and A. Suzuki, *Acta Mater.* **54**, 4953 (2006).
- [26] A. Karma, Z. T. Trautt, and Y. Mishin, *Phys. Rev. Lett.* **109**, 095501 (2012).
- [27] R. Lifshitz and D. M. Petrich, *Phys. Rev. Lett.* **79**, 1261 (1997).
- [28] K.-A. Wu, A. Adland, and A. Karma, *Phys Rev E* **81**, 061601 (2010).
- [29] Z. T. Trautt, A. Adland, A. Karma, and Y. Mishin, *Acta Mater.* **60**, 6528 (2012); Burgers vectors are defined here differently with respect to the crystal axes of the square lattice.
- [30] A. Adland, A. Karma, R. Spatschek, D. Buta, and M. Asta, *Phys. Rev.* **B87**, 024110 (2013).
- [31] See Supplemental Material.
- [32] W. J. Boettinger, J. A. Warren, C. Beckermann, and A. Karma, *Ann. Rev. Mater. Res.* **32**, 163 (2002).